iScience

CellPress
OPEN ACCESS

Article

Lipid droplets modulate proteostasis, SQST-1/SQSTM1 dynamics, and lifespan in *C. elegans*

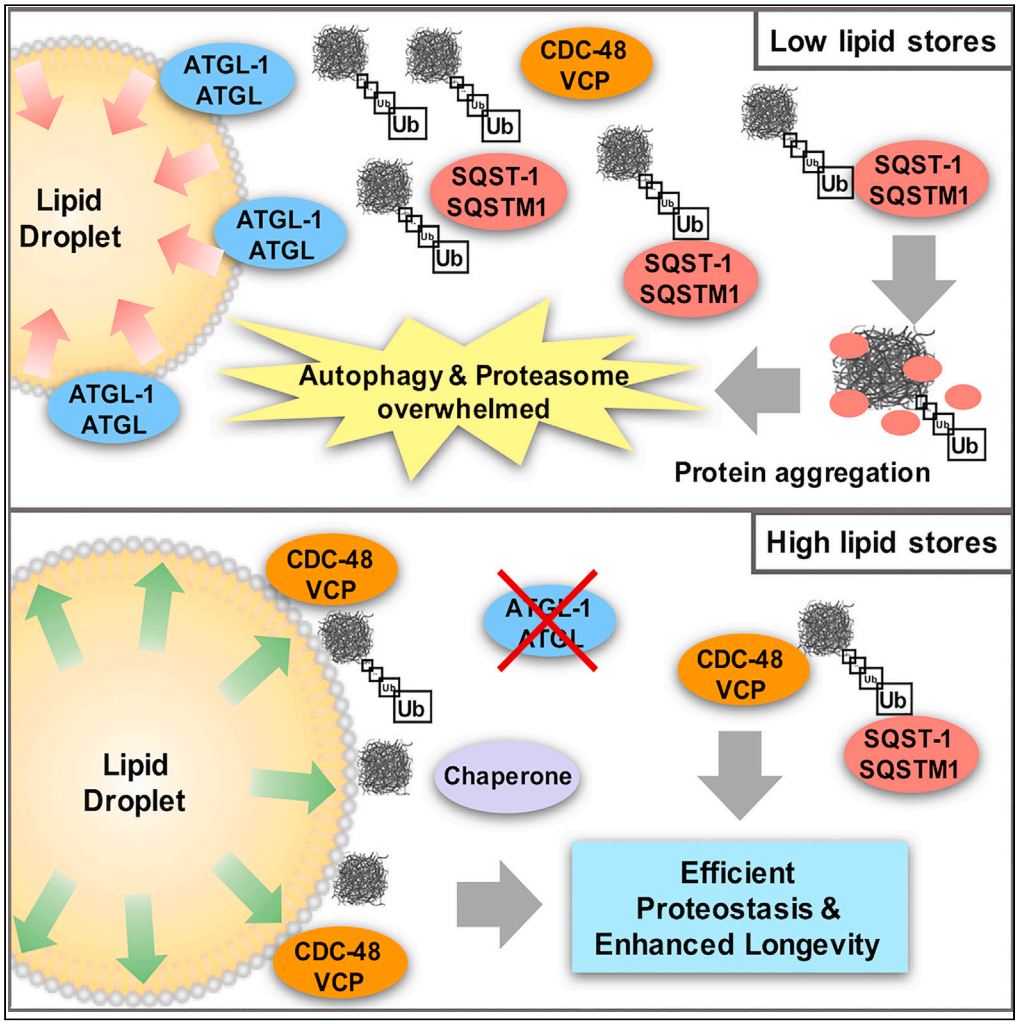

Anita V. Kumar, Joslyn Mills, Wesley M. Parker, ..., Joseph R. Johnson, Shi Quan Wong, Louis R. Lapierre

louis.rene.lapierre@umoncton.ca

Highlights

Elevated levels of SQST-1/SQSTM1 are detrimental to lifespan in *C. elegans*

Low lipid stores challenge the ability of SQST-1 to facilitate protein degradation

High lipid droplet content stabilizes aggregation-prone proteins

Age-related proteostatic decline is mitigated by lipid droplets

Kumar et al., iScience *26*, 107960
October 20, 2023
https://doi.org/10.1016/j.isci.2023.107960

iScience

CellPress
OPEN ACCESS

Article

Lipid droplets modulate proteostasis, SQST-1/SQSTM1 dynamics, and lifespan in *C. elegans*

Anita V. Kumar,[1,5] Joslyn Mills,[1,2,5] Wesley M. Parker,[1,5] Joshua A. Leitão,[1,5] Diego I. Rodriguez,[1] Sandrine E. Daigle,[3,4] Celeste Ng,[1] Rishi Patel,[1] Joseph L. Aguilera,[1] Joseph R. Johnson,[1] Shi Quan Wong,[1] and Louis R. Lapierre[1,3,4,6,*]

SUMMARY

In several long-lived *Caenorhabditis elegans* strains, such as insulin/IGF-1 receptor *daf-2* mutants, enhanced proteostatic mechanisms are accompanied by elevated intestinal lipid stores, but their role in longevity is unclear. Here, while determining the regulatory network of the selective autophagy receptor SQST-1/SQSTM1, we uncovered an important role for lipid droplets in proteostasis and longevity. Using genome-wide RNAi screening, we identified several SQST-1 modulators, including lipid droplets-associated and aggregation-prone proteins. Expansion of intestinal lipid droplets by silencing the conserved cytosolic triacylglycerol lipase gene *atgl-1/ATGL* enhanced autophagy, and extended lifespan. Notably, a substantial amount of ubiquitinated proteins were found on lipid droplets. Reducing lipid droplet levels exacerbated the proteostatic collapse when autophagy or proteasome function was compromised, and significantly reduced the lifespan of long-lived *daf-2* animals. Altogether, our study uncovered a key role for lipid droplets in *C. elegans* as a proteostatic mediator that modulates ubiquitinated protein accumulation, facilitates autophagy, and promotes longevity.

INTRODUCTION

One of the major hallmarks of aging is the accumulation of damaged proteins that progressively compartmentalize in inclusions and aggregates.[1] In the nematode *Caenorhabditis elegans*, numerous proteins display impaired solubility with age.[2,3] This phenomenon suggests that mechanisms that mediate proteostasis, such as chaperone-mediated folding and stabilization, actively contribute to somatic maintenance by preventing the collapse of the proteome.[4,5] The enhanced proteasomal[6] and autophagic[7,8] capacities, the increased chaperone function,[9] and alterations in ribosomal biogenesis[10] and function[11,12] in long-lived nematodes support the notion that the balance between synthesis, folding, and efficient clearance of proteins is important for conferring organismal longevity.

Generally, proteins destined for degradation are tagged via poly-ubiquitination and recognized by ubiquitin binding domain-containing proteins that direct cargo toward proteasomal or autophagic degradation. The autophagy receptor, Sequestosome-1 (SQST-1/SQSTM1) is a well-established and conserved mediator of cargo recognition, which includes ubiquitinated targets.[13] The SQST-1/SQSTM1-cargo complex can interact with the autophagosome proteins LGG-1/GABARAP and LGG-2/LC3 to enable cargo sequestration in the nascent autophagosome.[14] Notably, SQST-1/SQSTM1 has emerged as a potential lifespan modulator in nematodes and flies.[15–17] Additionally, selective autophagy of mitochondria has been linked to longevity,[18] suggesting that autophagic degradation of specific cargos and organelles is beneficial against organismal aging. Although SQST-1/SQSTM1 has been implicated in the selective clearance of aggregated proteins,[19] much remains to be understood about the modulation of this autophagy receptor, its cargoes, and the nature and extent of its contribution to lifespan.

In nematodes, intestinal cells have a unique role in autophagy-mediated longevity as they manage nutrient influx and signals from neurons[20] and the germline[21] to coordinate appropriate responses necessary for organismal survival. In particular, intestinal autophagy genes are required for lifespan extension[22] by maintaining intestinal tissue integrity and proteostasis. Intestinal cells are also sites of dynamic lysosomal function[23–26] that mediate specific longevity-associated lipid signaling.[27–29] Intriguingly, several established long-lived animals including insulin/IGF-1 receptor *daf-2*, germline-less *glp-1* and protein synthesis *rsks-1* mutants also maintain unusually large intestinal lipid droplet stores throughout their life.[30–33] Accordingly, redistributing lipids intended for secreted lipoproteins to intestinal lipid droplets is sufficient

[1]Department of Molecular Biology, Cell Biology and Biochemistry, Brown University, 185 Meeting Street, Providence, RI 02912, USA
[2]Biology Department, Wheaton College, 26 E. Main Street, Norton, MA 02766, USA
[3]New Brunswick Center for Precision Medicine, 27 rue Providence, Moncton, NB E1C 8X3, Canada
[4]Département de chimie et biochimie, Université de Moncton, 18 Antonine Maillet, Moncton, NB E1A 3E9, Canada
[5]These authors contributed equally
[6]Lead contact
*Correspondence: louis.rene.lapierre@umoncton.ca
https://doi.org/10.1016/j.isci.2023.107960

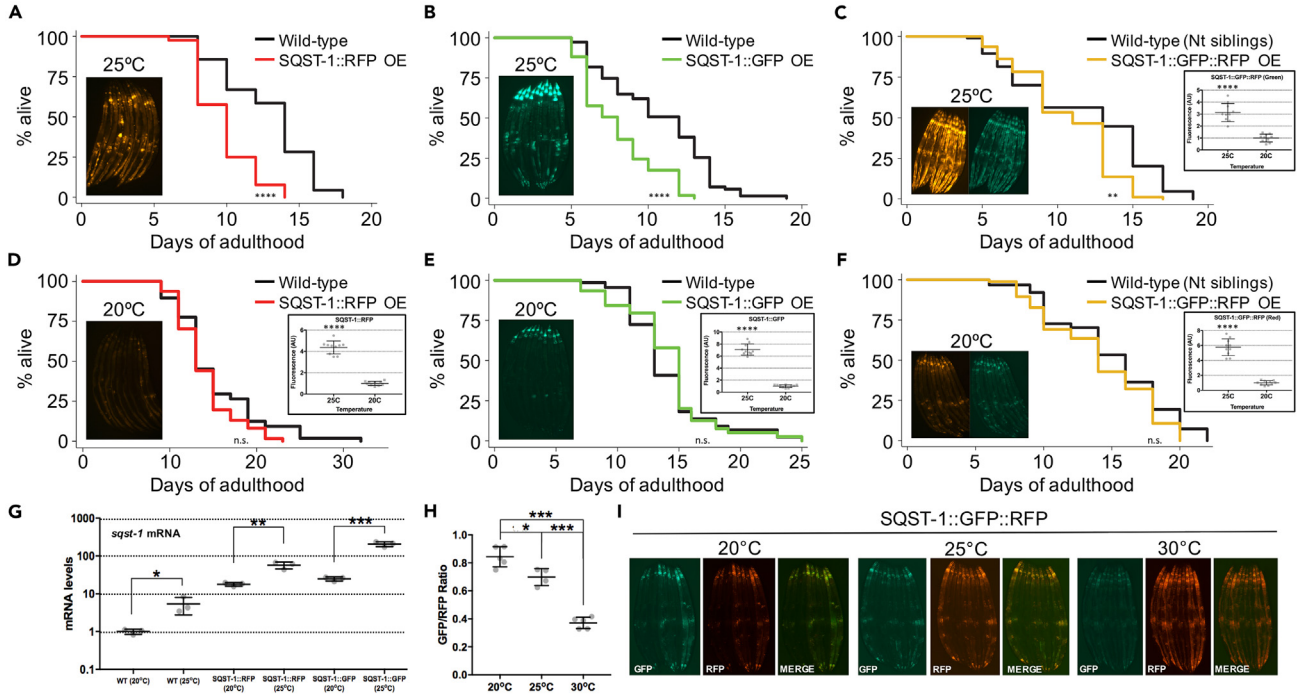

Figure 1. SQST-1 dynamics and lifespan modulation is temperature-dependent in *C. elegans*

(A–F) Lifespan analysis of wild-type animals and animals over-expressing SQST-1 fused to RFP, GFP or GFP::RFP fed OP50 *E. coli*, developmentally raised at 20°C and then grown at 25°C (A–C) or 20°C (D–F) during adulthood (n = 100). Insets include corresponding representative images of transgenic animals at Day 5 of adulthood, and quantified fluorescence, ±SD *t*-test ****p < *0.001*.

(G and H) (G) *sqst-1* mRNA levels in wild-type and transgenic animals were quantified by qPCR. Biological triplicates ±SD *t*-test *p < *0.05*, **p < *0.01*, ***p < *0.001* (H). Levels of GFP and RFP were measured in transgenic tandem SQST-1:GFP::RFP animals (leveraging the pH sensitivity of GFP to visualize SQST-1 accumulation in autolysosome) after incubating Day 1 animals at 20°C, 25°C or 30°C for 24 h. Average of 10 worms per image. n = 5 images per condition ±SD *ANOVA* *p < *0.05*, **p < *0.01*, ***p < *0.001*. Difference in signal between GFP and RFP is due to the low pH sensitivity of GFP. Thus, RFP-only signal represents SQST-1 protein in autolysosomes.

(I) Representative images of transgenic animals (quantified in h.) incubated at 20°C, 25°C or 30°C for 24 h. Details about lifespan analyses and repeats are available in Table S4, Mantel-Cox log rank. n.s.: not significant, **p < *0.01*,****p < *0.001*.

to extend lifespan.[29] However, in long-lived animals, it is unclear whether the maintenance of adult intestinal lipid stores is simply a consequence of reduced demand from the germline,[34] a long-term energy store rationing strategy[35] or a more direct mediator of somatic maintenance. Here, while identifying the regulatory network of SQST-1, we found that lipid droplet accumulation in long-lived nematodes represents a novel proteostatic mechanism that reduces overall SQST-1 and polyubiquitinated protein levels, and mitigates age-related proteostatic stress.

RESULTS

SQST-1 over-expression is detrimental to lifespan in *C. elegans*

We initially considered the possibility that increasing SQST-1 may improve proteostasis by enhancing the ability of cells to mediate selective autophagy. We hypothesized that increasing the expression of a receptor that recognizes ubiquitinated cargoes may suffice in driving their degradation. While this study was being conducted, the Hansen laboratory showed that over-expressing SQST-1 can extend lifespan at 20°C.[16] Since longevity interventions and temperature mechanistically interact,[36] we examined lifespan at both 20°C and 25°C using several over-expressing strains (*psqst-1::sqst-1::rfp*, *psqst-1::sqst-1::gfp::rfp*), including two created in the Hansen laboratory (*psqst-1::sqst-1::gfp* and *psqst-1::sqst-1*).[16] Over-expression of SQST-1 was unexpectedly detrimental at 25°C (Figures 1A–1C and S1A–S1C) and was not sufficient to extend lifespan at 20°C (Figures 1D–1F). While our findings at 20°C differ from recent literature,[16] highlighting potential lab-to-lab experimental variations, our findings are in line with most studies about the autophagy pathway and aging, i.e., that solely over-expressing an autophagy protein or an autophagy receptor might not necessarily be sufficient to improve lifespan.[37] At 25°C, SQST-1 clearly accumulates in the head, as well as the gonadal and intestinal tissues (Figure S1D) as previously reported.[38] A closer investigation into the temperature-dependent differences in lifespan revealed marked upregulation of *sqst-1* mRNA at higher temperature in these strains (from ~5-fold in wild-type, up to ~75-fold in SQST-1:GFP over-expressing animals) (Figure 1G). In order to measure the active trafficking of SQST-1 into the lysosome as a

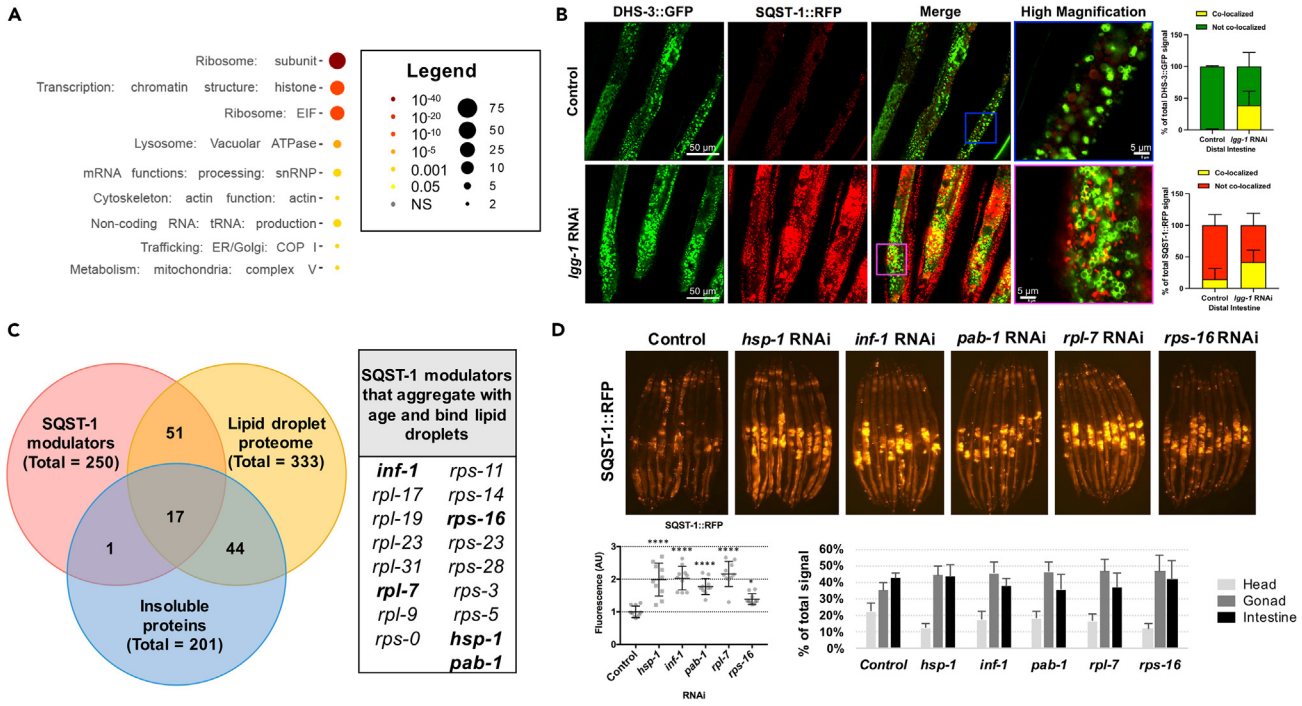

Figure 2. SQST-1 regulators include proteins that bind lipid droplets and that aggregate with age

(A) Pathway enrichment of genes that regulate SQST-1 levels using WormCat.[44]

(B) SQST-1:RFP accumulates after autophagy is inhibited by *lgg-1* silencing for 3 days during adulthood at 25°C. Representative confocal microscopy image of the distal intestine of animals expressing both SQST-1:RFP and the lipid droplet-resident protein DHS-3 fused to GFP, subjected to *lgg-1* silencing for 3 days during adulthood at 25°C. The co-localization between DHS-3:GFP and SQST-1:GFP is quantified.

(C) Overlap of SQST-1 regulators with age-dependent aggregating proteins[2] and lipid droplet-associated proteins.[40] Bolded genes were selected as representative.

(D) Representative images of gene silencing of a selected set of overlapping SQST-1 regulators during adulthood for 3 days at 25°C in animals over-expressing SQST-1:RFP. Fluorescence and tissue distribution quantified ±SD *ANOVA* *p < *0.05*,****p < *0.001*. Details about SQST-1 regulators are available in Tables S1 and S2.

guide for selective autophagy, we developed a tandem reporter system expressing SQST-1 fused to both GFP and RFP[7] (GFP signal is quenched in low pH environments). We confirmed that the conversion of tandem SQST-1 into an RFP-only signal is reduced in *lgg-1*- or *lgg-2*-silenced animals (Figure S1E) and autophagy-deficient *atg-18* mutants (Figure S1F). While relatively modest at 20°C (Figures 1H and 1I), increasing temperature up to 30°C for 24 h significantly enhanced the conversion to the RFP-only SQST-1 signal in the SQST-1 tandem reporter, suggesting that selective autophagy is induced with heat stress. Substantial temperature-dependent intestinal and neuronal accumulation of SQST-1 occurred during aging, and over-expressing SQST-1 at 25°C was also accompanied by higher levels of total polyubiquitinated proteins (Figures 1A–1F inset; S1G, and S1H). While over-expressing SQST-1 was detrimental at 25°C, so was the loss of *sqst-1* (Figures S1I and S1J), suggesting that SQST-1 function has a temperature-specific role in the lifespan of wild-type animals. Expression and steady-state levels of SQST-1 likely need to be tightly coordinated with cargo targeting and more importantly, with the rate of protein degradation systems (i.e., autophagy and proteasome). Altogether, we found that solely increasing SQST-1 is detrimental for lifespan at 25°C and inconsequential at 20°C, indicating a temperature-dependent effect on SQST-1 dynamics in aging.

Proteins that bind lipid droplets modulate SQST-1 dynamics

In order to better understand how SQST-1 is regulated, we opted for an unbiased genome-wide RNAi screening approach in an integrated SQST-1 over-expressing strain (*psqst-1::sqst-1::gfp*) at 25°C during development. SQST-1 modulators were subsequently validated by gene silencing in a separate over-expressing strain (*psqst-1::sqst-1::rfp*) during development and adulthood. Interestingly, the vast majority of modifiers led to the intestinal accumulation of fluorescently tagged SQST-1 in both development and adulthood (Table S1). A substantial portion of genetic modifiers clustered in ribosomal-related proteins, including proteins coding for small and large subunits, suggesting that ribosomal assembly and function substantially impact SQST-1 dynamics (Figure 2A; Table S1). This is in line with studies in *C. elegans*[2] and killifish,[39] highlighting the age-related instability of several ribosomal proteins and consequent ribosomal mis-assembly. Loss of ribosome subunit RPL-43 was also found to increase SQST-1 accumulation during development.[40] Since SQSTM1 was also recently reported to associate with lipid droplets in macrophages,[41] we wondered if SQST-1 might also associate with lipid droplets. We co-expressed SQST-1:RFP and the

lipid resident protein DHS-3 fused to GFP[42] in nematodes and we found that close to 50% of SQST-1:RFP localizes to lipid droplets when autophagy is inhibited (Figures 2B and S2A). Thus, we investigated whether SQST-1 modulators may also be related to lipid droplet metabolism. We compared our SQST-1 modulators to proteins that have been found to bind lipid droplets[43] and found significant overlap ($p < 5.745e-60$) (Figure 2C). Interestingly, several proteins prone to age-dependent aggregation[2] also modulated SQST-1 accumulation ($p < 6.030e-10$) (Figure 2C). Overall, 17 SQST-1 modulators have the propensity to both aggregate with age and bind lipid droplets (Figure 2C; Table S2). Several ribosomal subunits (*rps* and *rpl* genes) and mRNA-related proteins (*inf-1* and *pab-1*) emerged, along with the HSP70 chaperone family member *hsp-1/HSPA8*, indicating that ribosomal assembly, translation initiation, and protein folding are important regulators of SQST-1 dynamics (Figure 2D). SQST-1:RFP accumulation upon silencing of these modifiers was mostly gonadal and intestinal (Figures 2D and S2B). Interestingly, the expression of *sqst-1* was differentially regulated by the 17 SQST-1 modulators whereas silencing large ribosomal proteins generally increased *sqst-1* expression (Figure S2B). This observation highlights that *sqst-1* expression is potentially sensitive to ribosomal protein stoichiometry. Here, our comparative analysis suggests that age-related SQST-1 accumulation may be partly attributed to altered interactions between lipid droplets and progressively unstable protein complexes like the ribosome.

Elevated lipid droplets reduce SQST-1 accumulation and extend lifespan

Intestinal lipid droplet accumulation is a striking feature of several long-lived nematodes.[30–32] Since SQST-1 accumulated on lipid droplets when autophagy was inhibited (Figure 2B), and several SQST-1 modifiers bind lipid droplets (Figure 2C), we speculated that lipid droplets may underlie the ability of long-lived animals to stabilize or facilitate clearance of potentially aggregating proteins and maintain proteome stability during aging. In order to specifically stimulate intestinal lipid droplet accumulation, we silenced the conserved cytosolic lipase *atgl-1/ATGL*[45] during adulthood to attenuate lipid droplet breakdown, which led to significantly larger lipid stores (+47% $\pm$ 20%), thereby mimicking a key feature of several established long-lived nematodes[30–33] (Figure 3A, inset). Silencing *atgl-1* resulted in a significant lifespan extension in wild-type animals (12–28%), indicating that lipid droplet accumulation is sufficient to mediate longevity (Figures 3A and 3B). Silencing ATGL-1 activator *lid-1* or hormone-sensitive lipase orthologue *hosl-1*[46] during adulthood also led to similar reduction in SQST-1 accumulation and lifespan extension as observed with *atgl-1* silencing (Figures S2C and S2D). These observations pointed to a possible lipid droplet-mediated cytoprotective mechanism.[47] Indeed, silencing *atgl-1* in SQST-1:RFP over-expressing animals led to a substantial increase in lifespan (Figure 3C) accompanied by a marked decrease in SQST-1 accumulation (Figure 3D). Similar observations were made in animals over-expressing SQST-1:GFP (Figure S2E), suggesting that the lipid droplet-mediated effects impacts SQST-1-mediated selective autophagy.

To determine whether accumulation of lipids is able to improve the lifespan of proteostatically impaired mutants, we silenced *atgl-1* in three well-established short-lived mutants, including *daf-16(mu86)*, *hlh-30(tm1978)*, and *hsf-1(sy441)*.[48] Notably, the expression of these transcription factors was increased at 25°C compared to 20°C, suggesting that their function may be stimulated by heat (Figure S2F). Silencing *atgl-1* extended the lifespan of *daf-16* and *hlh-30* mutants, but not the lifespan of *hsf-1* mutants (Figures 3E–3G), indicating that lipid droplet-mediated lifespan extension may require the expression of key chaperones regulated by HSF-1/HSF1, such as heat shock protein HSP-1, which binds lipid droplets and modulates SQST-1 levels (Figure 2D). Interestingly, lipid droplets may harbor chaperones with roles in aggregate clearance.[49] Notably, autophagic activity, as measured by the tandem mCherry:GFP::LGG-1 reporter,[7] showed that *atgl-1* silencing increases the conversion of autophagosomes (GFP+mCherry - yellow puncta) into autolysosomes (mCherry only - red puncta) (Figures 3H and S2G). Accordingly, the lifespan of autophagy-deficient *atg-7* mutants was not increased by silencing *atgl-1* (Figure S2H).

As our lifespan analyses highlighted novel proteostatic and longevity roles for lipid droplets, we reasoned that long-lived animals with large lipid stores should accumulate less intestinal SQST-1. Strikingly, *daf-2(e1370)* expressing SQST-1:GFP (Figure 3I) or SQST-1:RFP (Figure S2I) accumulated negligible intestinal SQST-1 during aging (GFP signal in mid-section was entirely gonadal, see wild-type comparison in Figure 1B). In addition, SQST-1 over-expression did not significantly affect the long lifespan of *daf-2* animals (Figure 3I). Loss of *sqst-1* did not affect the lifespan of *daf-2* animals (Figure S2J), as previously shown,[16] highlighting that SQST-1 function becomes less important at 25°C for the lifespan of organisms with relatively stable proteomes and high lipid stores. The extent of heat-induced increase in SQST-1-mediated selective autophagy was also attenuated in *daf-2* animals (Figure S2K) compared to wild-type (Figure 1H), suggesting that elevated lipid droplets may buffer the need for SQST-1 function during heat stress. Silencing *atgl-1* in *daf-2* animals enhanced their intestinal lipid stores and further extended their lifespan (Figure 3J), indicating that elevated lipid droplet accumulation can also extend lifespan in animals with enhanced proteostasis. Altogether, our data present an important and previously unrecognized role for lipid droplets in SQST-1 dynamics and longevity.

Silencing atgl-1 elicits limited changes in gene expression

Lipid droplets have been recently shown to coordinate transcriptional programs by sequestering factors that modulate transcription.[50] Since HSF-1 was required for lifespan extension by *atgl-1* silencing, we hypothesized that the lipid droplet increase associated with *atgl-1* silencing might affect the expression of HSF-1-regulated targets. Using RNA sequencing (RNA-seq), we found that enhancing lipid stores by silencing *atgl-1* in WT or *daf-2* animals had limited effect on global transcription. Silencing *atgl-1* resulted in 13 overlapping differentially expressed genes (DEG) in wild-type animals and *daf-2* mutants of which 6 genes besides *atgl-1* are down-regulated in both cases (Figures S3A and S3B). The mRNA levels of *sqst-1* remained unchanged by *atgl-1* silencing (Figure S3C). Altering *atgl-1* levels (silencing or over-expression) led to differential expression of 50 overlapping genes, with no discernable transcription factor signature (Figures S3D and S3E). In addition, expression of *sqst-1* was unchanged in wild-type animals with low or high levels of *atgl-1* (Figure S3E). Overall, we concluded that

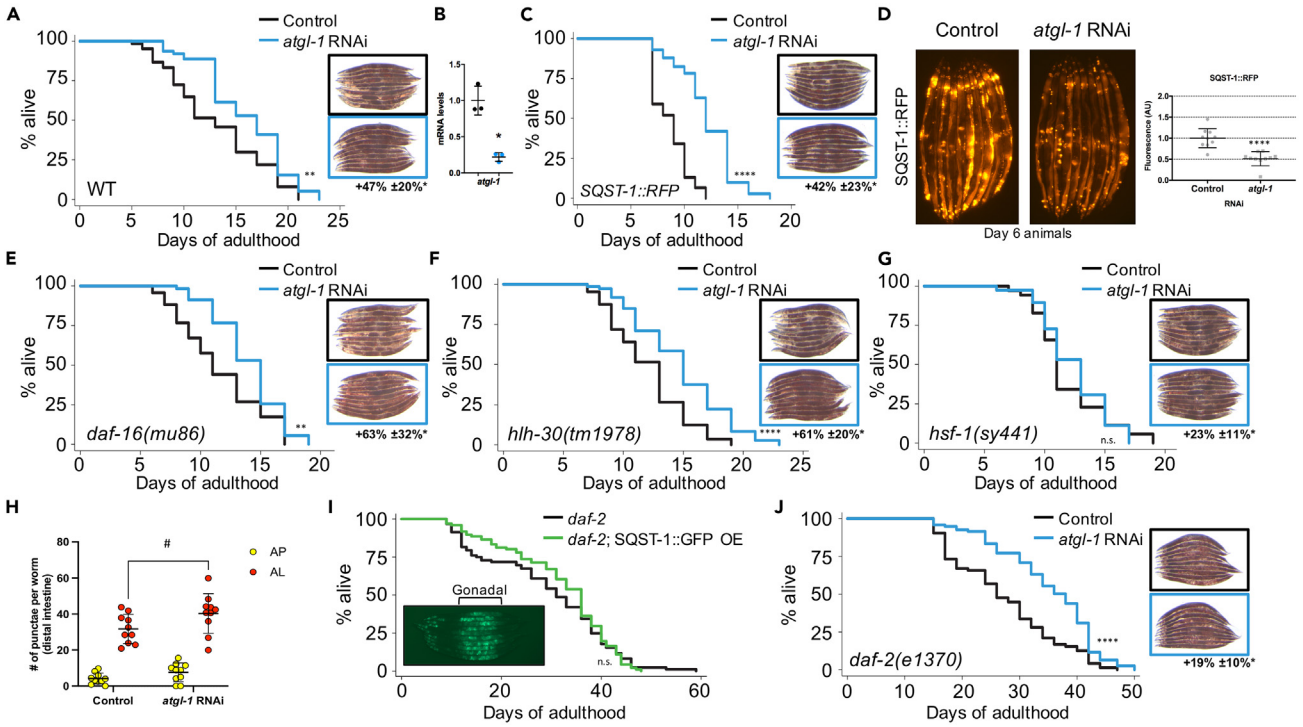

Figure 3. Silencing *atgl-1* extends lifespan and reduces SQST-1 accumulation in *C. elegans*

(A and C) (A) Lifespan analysis of wild-type animals and (C). animals over-expressing SQST-1:RFP raised at 20°C on OP50 *E. coli* and then grown at 25°C during adulthood on control bacteria or bacteria expressing dsRNA against *atgl-1* (n = 100). Corresponding images of Day 5 animals stained with Oil Red O demonstrating intestinal lipid store accretion under *atgl-1* RNAi (blue borders), with quantification below. n = 10 *t*-test *p < *0.05*.

(B and D) (B) Levels of *atgl-1* mRNA measured by qPCR showing efficient silencing after 3 days on *atgl-1* RNAi (Black: Control RNAi, Blue: *atgl-1* RNAi). Biological triplicates *t*-test *p < *0.05* (D). Representative fluorescence images taken after Day 1 animals over-expressing SQST-1:RFP and DHS-3:GFP were fed control bacteria or bacteria expressing dsRNA against *atgl-1* for 5 days at 25°C.

(E–G) Lifespan analysis of *daf-16(mu86)*, *hlh-30(tm1978)*, and *hsf-1(sy441)* mutants raised at 20°C on OP50 *E. coli* and then grown at 25°C during adulthood on control bacteria or bacteria expressing dsRNA against *atgl-1* (n = 100). Corresponding images of Day 5 animals stained with ORO demonstrating intestinal lipid store accretion under *atgl-1* RNAi (blue borders).

(H and I) (H) Levels of autophagosomes and autolysosomes were measured in animals expressing the tandem reporter mCherry:GFP::LGG-1[7] after feeding Day 1 animals with control bacteria or bacteria expressing dsRNA against *atgl-1* for 2 days at 25°C. n = 10 per condition ± SD *t*-test #p < *0.06* (I). Lifespan analysis of *daf-2(e1370)* and *daf-2;SQST-1::GFP* animals raised at 20°C and then grown at 25°C during adulthood on OP50 *E. coli* (with representative image of Day 5 animals, comparative image of wild-type animals in Figure 1B).

(J) *daf-2(e1370)* animals were raised at 20°C on OP50 *E. coli* and then grown at 25°C during adulthood on control bacteria or bacteria expressing dsRNA against *atgl-1* (n = 100). Corresponding images of Day 5 animals stained with ORO demonstrating intestinal lipid store accretion under *atgl-1* RNAi (blue borders). Details about lifespan analyses and repeats are available in Tables S3 and S4, Mantel-Cox log rank. n.s.: not significant, **p < *0.01*,****p < *0.001*.

transcriptional regulation may not contribute significantly to the proteostatic-enhancing and lifespan-extending effects of lipid droplets. Therefore, lipid droplets may impact proteostasis via a more direct mechanism on the proteome itself.

Lipid droplets enhance proteostasis by modulating the accumulation of ubiquitinated proteins

The emerging connection between lipid droplet stores and proteome stability led us to investigate how lipid droplet loss affects proteostasis and SQST-1 abundance. First, we tested whether lipid droplet depletion affects lifespan using ATGL-1:GFP over-expressing animals.[51] Opposite of the effect observed at 20°C (Table S3),[52] we found that over-expressing ATGL-1 was detrimental to lifespan at 25°C (Figure 4A) and led to a significant increase in SQST-1 intestinal accumulation accompanied by lower lipid stores (Figure 4B), suggesting that loss of lipid droplet stores can interfere with SQST-1 dynamics. When autophagy or proteasome function was reduced by silencing autophagosome protein *lgg-1* or proteasome subunit *rpn-6.1*, respectively, ubiquitinated protein levels were higher in animals with lower lipid stores, suggesting that lipid droplets may buffer the proteome and facilitate the processing of unstable or misfolded proteins (Figures 4C and S4A). Strikingly, analyzing lipid droplets revealed substantial accumulation of ubiquitinated proteins in lipid droplet-enriched fractions (Figures 4D and S4B), indicating that lipid droplets contain a significant amount of proteins potentially bound for degradation. Lipid droplet-associated accumulation of ubiquitinated proteins was increased when autophagic or proteasomal degradation was reduced (Figure 4D), suggesting that lipid droplets have

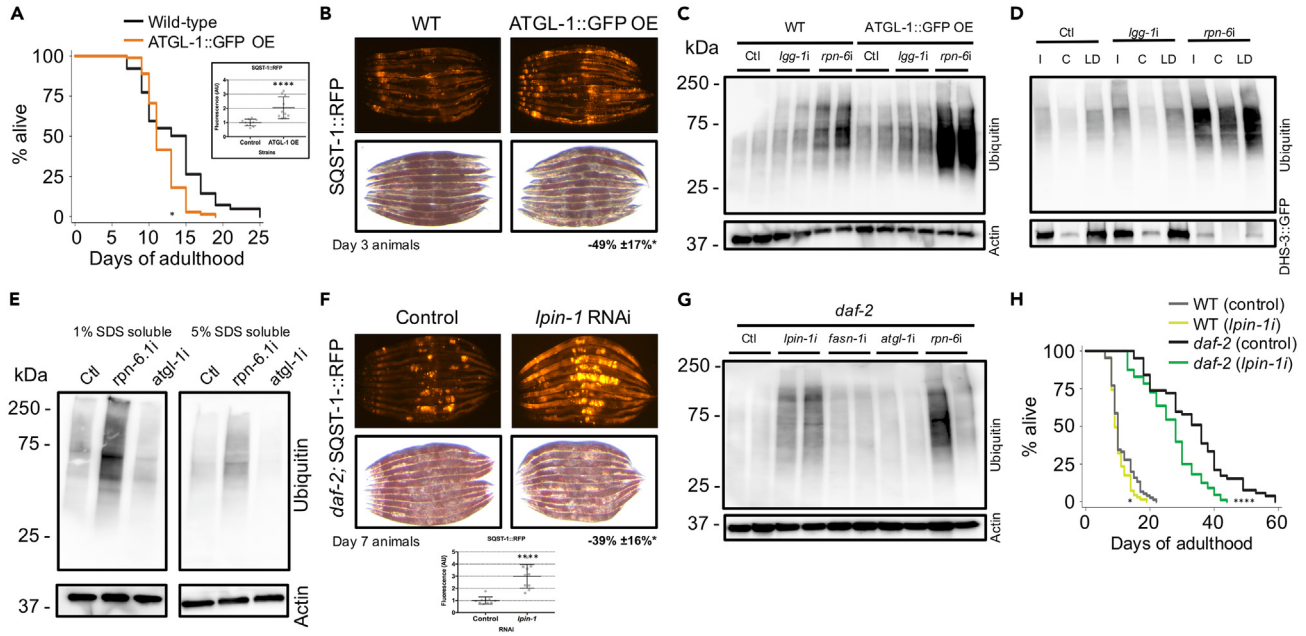

Figure 4. Lipid droplets modulate ubiquitinated protein accumulation, SQST-1 levels, and lifespan

(A) Lifespan analysis of wild-type and transgenic animals over-expressing ATGL-1:GFP developmentally raised at 20°C and then grown at 25°C during adulthood on OP50 *E. coli* (n = 100).

(B) Levels of RFP signal and lipid droplets from Day 3 animals over-expressing SQST-1:RFP in wild-type or transgenic ATGL-1:GFP over-expressing background.

(C) Wild-type and ATGL-1:GFP over-expressing animals were raised at 20°C and then grown at 25°C during adulthood on control bacteria (Ctl) or bacteria expressing dsRNA against autophagy gene *lgg-1* or proteasome subunit gene *rpn-6.1* for 2 days. Levels of ubiquitinated proteins and actin were visualized by immunoblotting. Actin was used as loading control. Biological replicates shown.

(D) Animals expressing lipid droplet-resident protein DHS-3 fused to GFP were raised at 20°C and then grown at 25°C during adulthood on control bacteria or bacteria expressing RNAi against *lgg-1* or *rpn-6* for 4 days. Levels of ubiquitinated proteins and DHS-3:GFP were visualized by immunoblotting from total input (I), cytosol (C) and lipid droplet (LD) fractions (comparative % loaded between fractions, i.e., 10%).

(E) Day 1 wild-type animals were fed control bacteria or bacteria expressing dsRNA against *rpn-6* or *atgl-1* for 3 days and ubiquitination levels were detected by immunoblotting.

(F) Levels of RFP signal and lipid droplets in Day 7 *daf-2* animals over-expressing SQST-1:RFP and fed control bacteria or bacteria expressing dsRNA against *lpin-1* during adulthood.

(G) Day 1 *daf-2* animals were fed control bacteria or bacteria expressing dsRNA against *atgl-1*, *rpn-6* or *lpin-1* for 5 days at 25°C and ubiquitination levels were detected by immunoblotting. Actin was used as loading control. Biological replicates shown.

(H) Lifespan analysis of wild-type and *daf-2(e1370)* raised at 20°C on OP50 *E. coli* and then grown at 25°C during adulthood on control bacteria or bacteria expressing dsRNA against *lpin-1* (n = 100). Details about lifespan analyses and repeats are available in Tables S3 and S4, Mantel-Cox log rank. n.s.: not significant, *p < *0.05*,****p < *0.001*.

the capacity to harbor many degradation cargoes, which may become particularly relevant for proteostasis when autophagic and proteasomal systems are failing during aging.

The association and function of ATGL-1 with lipid droplets was recently found to be antagonized by the AAA-ATPase CDC-48/VCP.[53] CDC-48/VCP is best known for its role in ER-associated degradation machinery,[54] but it has been associated with other functions including endocytosis[55] and more recently autophagy itself.[56] CDC-48/VCP helps unfold unstable, ubiquitinated, and proteasomal degradation-bound proteins in concert with heat shock protein HSP-70, a key regulated target of HSF-1.[57] Thus, we assayed the effect of the loss of CDC-48 on SQST-1 and ATGL-1 levels using fluorescent reporters. Silencing *cdc-48.2* increased the levels of ATGL-1:GFP (Figure S4C) and led to the accumulation of SQST-1:RFP (Figure S4D). In mammalian cells, loss of proteasome function drives SQSTM1 to divert cargo to selective autophagy,[58] but stimulating proteasomal processing by over-expressing of VCP can reduce SQSTM1 accumulation.[59] Here, we reasoned that CDC-48 functions related to processing ubiquitinated targets and autophagy may underlie the ability of nematodes with elevated lipid droplets to attenuate SQST-1 accumulation and modulate lifespan. Accordingly, silencing *atgl-1* in *cdc-48.1* or *cdc-48.2* mutants failed to significantly extend lifespan (Figure S4E; Table S4), indicating that lipid droplet-mediated lifespan extension requires functional CDC-48.

As lipid droplet size increases, its surface also increases, and it is possible that the capacity of this organelle to bind and stabilize proteins may also increase as well. Enhancing lipid droplet stores by silencing *atgl-1* reduced the overall accumulation of ubiquitinated proteins, in particular in the lower solubility (5% SDS soluble) fraction (Figure 4E), suggesting that typically insoluble proteins are less likely to be

ubiquitinated when lipid droplets abound. Notably, the types of proteins that aggregate with age differ between wild-type and long-lived *daf-2* mutants, as the latter tends to accumulate aggregating proteins that are less hydrophobic than those aggregating in wild-type animals.[4] Reducing lipid droplet stores genetically by silencing lipogenic genes *sbp-1(SREBP2)*, *lpin-1(LIPN1)* or *fasn-1(FASN)* enhanced SQST-1 accumulation in wild-type animals (Figure S4F). Similarly, loss of lipid droplet stores by silencing *lpin-1* in *daf-2* resulted in increased SQST-1 accumulation and overall protein ubiquitination (Figures 4F, 4G, and S4G). Ultimately, in wild-type and more significantly in *daf-2* animals, silencing of *lpin-1* reduced their lifespan (Figure 4H). As proteostasis failure is a feature of neurodegeneration, we tested the effect of increasing lipid droplet levels in proteotoxic contexts. Animals intestinally expressing an aggregating poly-glutamine protein fused to YFP (Q44:YFP)[60] had reduced numbers of aggregates when *atgl-1* was silenced (Figure S4H). Reducing the expression of *atgl-1* in a muscle-expressing proteotoxic amyloid protein Aβ-42 resulted in a marked protection against aggregation-associated paralysis[61] (Figure S4I). Altogether, our data demonstrate that lipid droplets are important for proteostasis and contribute to lifespan by facilitating autophagy and stabilizing the proteome.

DISCUSSION

Decades of aging research has uncovered key longevity-regulating pathways in *C. elegans*,[48] yet the role of lipid droplets in the lifespan extension of several established long-lived nematodes has remained unresolved. Here, while studying the regulation of the selective autophagy receptor SQST-1, we unexpectedly uncovered a direct role for lipid droplets in proteostasis and lifespan. Several SQST-1 modulators associate with lipid droplets and aggregate with age, including ribosomal, translation-related, and folding-related proteins.[43] Ribosomal assembly dysfunction due to loss in subunit stoichiometry may burden the autophagy machinery, and contribute to age-related proteotoxicity.[39] Importantly, lipid droplet accumulation, by silencing cytosolic triacylglycerol lipase *atgl-1/ATGL*, mitigates the progressive age-related SQST-1 accumulation, a benefit recapitulated in long-lived, lipid droplet-rich *daf-2* mutant animals. Lipid droplets are cytoprotective as they prevent aberrant SQST-1 accumulation, in part via the functioning of AAA-ATPase CDC-48/VCP which processes ubiquitinated proteins for proteasomal degradation.[62] Strikingly, we found that a substantial portion of soluble ubiquitinated proteins in nematodes was associated with lipid droplets, suggesting that unstable proteins bound for degradation may be stabilized by the surface of lipid droplets. Our findings also provide support to the importance of the emerging lipid-droplet-mediated protein degradation process[63,64] in longevity and aging. Altogether, our study strengthens the emerging concept that lipid droplets serve as a buffer for proteostasis[47] by stabilizing proteomes and coordinating protein degradation machineries.

Understanding the regulation of SQST-1/SQSTM1 during aging and in different disease contexts is important in order to determine the validity of stimulating SQSTM1-mediated selective autophagy as a therapeutic strategy to improve proteostasis in age-related diseases.[65] Here, we find that over-expressing SQST-1 had no effect on the lifespan of wild-type animals at 20°C[16] whereas elevated SQST-1 level at 25°C was detrimental. While lab-to-lab variations in lifespan analyses can occur, we tested a variety of over-expressing strains for SQST-1 with different tags in order to more broadly assess the impact of high levels of SQST-1 on longevity. In hindsight, one could have predicted that over-expressing a ubiquitin-binding protein with a propensity for oligomerization with ubiquitinated cargoes[66] might not be necessarily advantageous. This is particularly relevant in *C. elegans* which is characterized by a proteome nearing its solubility limit[2,3] and displaying overall proteome instability and aggregated protein accumulation during aging.[5] SQST-1 over-expression was primarily visible in neuronal, gonadal and intestinal cells and accumulated in a temperature-dependent manner and progressively during aging. The inability of stressed and aging animals to process ubiquitinated cargos bound for proteasomal or autophagic degradation may lead to a gradual build-up of SQST-1. Accordingly, SQST-1 over-expression may over-sensitize the animals to unstable, ubiquitination-prone proteins, posing an additional challenge to the autophagic machinery. This is exemplified by recent evidence that reducing SQST-1 specifically in the neurons of a nematode model of ALS is protective,[67] possibly since mutant FUsed in Sarcoma (FUS) expression promotes SQST-1 accumulation, which exacerbates proteotoxicity and neurodegeneration. Notably, SQSTM1 can phase separate when interacting with ubiquitinated cargoes,[68] but the impact of the formation of these condensates on overall proteostasis is unclear.

Lipid droplet accumulation is a prominent and under-explored phenotype of several long-lived nematodes, including well-established models such as insulin/IGF-1 receptor *daf-2* mutants, germline-less *glp-1* animals and protein synthesis *rsks-1* mutants,[69] as well as in long-lived animals with reduced nuclear protein export.[70] In addition, lifespan extension by inhibiting intestinal lipid secretion mediated by vitellogenins results in lipid redistribution to intestinal lipid droplet stores,[29] a process believed to generate precursors for lysosomally-derived lipid signals.[28] While enhanced lysosomal lipolysis and lipophagy may stimulate longevity-associated lipid signaling, we found that overactive cytosolic lipolysis decreases the ability of cells to maintain a stable proteome, which may burden the selective autophagy machinery. Our findings support that lipid droplets are much more than just lipid storage organelles[47] and can serve as interfaces to enable protein stabilization and processing.

Rationing of intestinal lipid stores was originally evoked as a potential mechanism to provide long-term energy for dauer larvae that arrest feeding.[35] Here, we propose a role for lipid stores during adulthood that focuses on their capacity to buffer proteostasis during aging in concert with HSF-1 and heat shock chaperones, thereby unburdening protein degradation systems. ATGL-1 over-expression leads to lipid store depletion,[52] but, more importantly, it also removes the protection conferred by lipid droplets and renders animals vulnerable to proteotoxic stress associated with reduced proteasomal function, heat and aging. Thus, regulating the activity of ATGL-1 via transcription,[71] post-translational modification,[72] or alterations in CDC48/VCP activity[53] provide a mechanism by which cells modify protein homeostasis. Overall, our data show that the lipid droplet-mediated decrease in protein ubiquitination and the enhancement in lifespan require the function of the AAA-ATPase CDC-48/VCP, a ubiquitin protein processing enzyme and autophagy modulator.[56]

Lipid droplet expansion and accumulation may belong to an arsenal of proteostatic measures that lipid-storing cells and possibly neurons can employ to prevent protein misfolding and aggregation. While lipid droplet accumulation in immune cells such as macrophages[73] and microglia[74] may be inflammatory and contribute to aging, lipid droplets may confer some post-mitotic, terminally differentiated cells with added protection against protein aggregation[49] and mitochondrial lipid overload.[75] For example, lipid droplet accumulation in Alzheimer's disease pathogenesis[76] may highlight an effort from neuronal cells to improve proteome stability and resilience against progressive proteotoxicity. Notably, drastic inhibition of triacylglycerol lipolysis becomes detrimental to neurons[77] as larger lipid droplets are less easily broken down.[51] However, a recent study showed that lipid droplet accumulation protected hyper-activated neurons from cell death,[44] a phenomenon potentially relevant in Alzheimer's disease.[78] Thus, moderate accumulation of lipid droplets may be more desirable to provide protection against age-related proteotoxicity. In agreement, our data show marked protection against paralysis in a proteostatic Alzheimer's disease model by attenuating cytosolic lipolysis.

Enhancing proteostasis by stimulating the autophagy process has emerged as an attractive strategy to mitigate several age-related diseases with pathological proteostatic decline such as neurodegenerative diseases.[79] However, our study indicates that stimulating selective autophagy by specifically increasing the expression of one selective autophagy receptor, SQST-1/SQSTM1, is not sufficient to improve proteostasis and may exacerbate age-related proteostatic collapse. Overall, our study suggests that therapeutic improvement in proteostasis may benefit from a combinatorial approach in which the whole autophagy/lysosomal machinery is stimulated concomitantly with a modest reduction in lipid droplet breakdown. Such an approach may prevent pathogenic burdening of the autophagy/lysosome pathway with cargoes that could have otherwise been stabilized by lipid droplets or routed to the proteasome.

Limitations of the study

Our study uncovered novel regulators of SQST-1/SQSTM1 dynamics and place lipid droplets as an important organelle in SQST-1/SQSTM1 dynamics and ubiquitinated protein metabolism. Here, lifespan studies in SQST-1 transgenic animals were repeated with integrated and non-integrated stains, and with different tags, which improved confidence in our interpretations. Our findings highlight challenges that can arise with nematode lifespan studies, including variations across laboratories and the role that temperature can play in the study of proteins in transgenic strains that respond to temperature at the transgene expression level and dynamically at the protein level. Notably, modulating lipid droplet levels using gene silencing (*atgl-1*, *hosl-1* or *lid-1* RNAi) and long-lived *daf-2* mutants led to a substantial reduction in SQST-1 accumulation. Whether other nematode longevity models accumulate less SQST-1 with age could be tested in strains with high lipid droplet content, such as the germline-less *glp-1* animals and the protein synthesis *rsks-1* mutants. Also, we found interesting new roles of ribosomal subunits in SQST-1 accumulation which could be further clarified by studying the direct impact of ribosomal assembly and function on selective autophagy. Overall, while the mechanism by which lipid droplets modulate SQST-1/SQSTM1 dynamics and polyubiquitinated protein levels is not fully elucidated, our work lays the foundation to further study the role of lipid droplets in proteostasis and aging at the cellular, tissular, and organismal levels.

STAR★METHODS

Detailed methods are provided in the online version of this paper and include the following:

- KEY RESOURCES TABLE
- RESOURCE AVAILABILITY
  - Lead contact
  - Materials availability
  - Data and code availability
- EXPERIMENTAL MODEL AND STUDY PARTICIPANTS
  - *C. elegans* strain maintenance
  - Transgenic strain construction
- METHOD DETAILS
  - Genome-wide RNAi screen
  - Lifespan analyses
  - Comparative analyses
  - Imaging and analyses
  - Lipid staining
  - Gene expression analysis
  - RNAseq sample preparation and analysis
  - Lipid droplet fractionation
  - Immunoblotting
- QUANTIFICATION AND STATISTICAL ANALYSIS

SUPPLEMENTAL INFORMATION

Supplemental information can be found online at https://doi.org/10.1016/j.isci.2023.107960.

ACKNOWLEDGMENTS

We are grateful for the technical support provided by Erin McConnell, Rachel Tam and Tuong Tran. We thank the Malene Hansen laboratory (SBPMDI) and the Caenorhabditis Genetics Center (U. Minnesota, P40 OD010440) for providing transgenic and mutant strains and the Andrew Dillin laboratory (UC Berkeley/HHMI) for sharing expression plasmids. This work was funded by grants from the National Institutes of Health (R00 AG042494, R01 AG051810 and R21 AG068922), a Glenn Award for Research in Biological Mechanisms of Aging from the Glenn Foundation for Medical Research, an NSERC Discovery Grant and a Research Chair in Precision Medicine (J-Louis Lévesque Foundation - Research NB) to LRL.

AUTHOR CONTRIBUTIONS

A.V.K., J.M., W.M.P., and J.A.L. performed lifespan analyses and imaging as well as RNAi sequencing, validation, and analysis. A.V.K., J.M., J.A.L., and J.R.J. validated the whole-genome RNAi screening. J.M. performed the RNA sequencing and lipid droplet analyses. W.M.P. conducted lipid staining and A.V.K. performed the confocal microscopy imaging. D.I.R. performed RNAi sequencing and conducted qPCR analyses. S.D., C.N., R.P., and J.L.A. performed lifespan analysis repeats. S.Q.W. and W.M.P. developed SQST-1 over-expressing and tandem reporter strains. L.R.L. designed the experiments, conducted initial RNAi screening, imaging, qPCR and lifespan analyses, and wrote the manuscript. All co-authors edited the manuscript.

DECLARATION OF INTERESTS

None declared.

Received: September 5, 2022
Revised: June 1, 2023
Accepted: September 14, 2023
Published: September 16, 2023

REFERENCES

1. Koga, H., Kaushik, S., and Cuervo, A.M. (2011). Protein homeostasis and aging: The importance of exquisite quality control. Ageing Res. Rev. *10*, 205–215.
2. Reis-Rodrigues, P., Czerwieniec, G., Peters, T.W., Evani, U.S., Alavez, S., Gaman, E.A., Vantipalli, M., Mooney, S.D., Gibson, B.W., Lithgow, G.J., and Hughes, R.E. (2012). Proteomic analysis of age-dependent changes in protein solubility identifies genes that modulate lifespan. Aging Cell *11*, 120–127.
3. Sui, X., Pires, D.E.V., Ormsby, A.R., Cox, D., Nie, S., Vecchi, G., Vendruscolo, M., Ascher, D.B., Reid, G.E., and Hatters, D.M. (2020). Widespread remodeling of proteome solubility in response to different protein homeostasis stresses. Proc. Natl. Acad. Sci. USA *117*, 2422–2431.
4. Walther, D.M., Kasturi, P., Zheng, M., Pinkert, S., Vecchi, G., Ciryam, P., Morimoto, R.I., Dobson, C.M., Vendruscolo, M., Mann, M., and Hartl, F.U. (2015). Widespread Proteome Remodeling and Aggregation in Aging C. elegans. Cell *161*, 919–932.
5. Ben-Zvi, A., Miller, E.A., and Morimoto, R.I. (2009). Collapse of proteostasis represents an early molecular event in Caenorhabditis elegans aging. Proc. Natl. Acad. Sci. USA *106*, 14914–14919.
6. Vilchez, D., Morantte, I., Liu, Z., Douglas, P.M., Merkwirth, C., Rodrigues, A.P.C., Manning, G., and Dillin, A. (2012). RPN-6 determines C. elegans longevity under proteotoxic stress conditions. Nature *489*, 263–268.
7. Chang, J.T., Kumsta, C., Hellman, A.B., Adams, L.M., and Hansen, M. (2017). Spatiotemporal regulation of autophagy during Caenorhabditis elegans aging. Elife *6*, e18459.
8. Lapierre, L.R., De Magalhaes Filho, C.D., McQuary, P.R., Chu, C.C., Visvikis, O., Chang, J.T., Gelino, S., Ong, B., Davis, A.E., Irazoqui, J.E., et al. (2013). The TFEB orthologue HLH-30 regulates autophagy and modulates longevity in Caenorhabditis elegans. Nat. Commun. *4*, 2267.
9. Morley, J.F., and Morimoto, R.I. (2004). Regulation of longevity in Caenorhabditis elegans by heat shock factor and molecular chaperones. Mol. Biol. Cell *15*, 657–664.
10. Tiku, V., Jain, C., Raz, Y., Nakamura, S., Heestand, B., Liu, W., Späth, M., Suchiman, H.E.D., Müller, R.U., Slagboom, P.E., et al. (2017). Small nucleoli are a cellular hallmark of longevity. Nat. Commun. *8*, 16083.
11. Visscher, M., De Henau, S., Wildschut, M.H.E., van Es, R.M., Dhondt, I., Michels, H., Kemmeren, P., Nollen, E.A., Braeckman, B.P., Burgering, B.M.T., et al. (2016). Proteome-wide Changes in Protein Turnover Rates in C. elegans Models of Longevity and Age-Related Disease. Cell Rep. *16*, 3041–3051.
12. Dhondt, I., Petyuk, V.A., Cai, H., Vandemeulebroucke, L., Vierstraete, A., Smith, R.D., Depuydt, G., and Braeckman, B.P. (2016). FOXO/DAF-16 Activation Slows Down Turnover of the Majority of Proteins in C. elegans. Cell Rep. *16*, 3028–3040.
13. Kirkin, V., and Rogov, V.V. (2019). A Diversity of Selective Autophagy Receptors Determines the Specificity of the Autophagy Pathway. Mol. Cell *76*, 268–285.
14. Pankiv, S., Clausen, T.H., Lamark, T., Brech, A., Bruun, J.A., Outzen, H., Øvervatn, A., Bjørkøy, G., and Johansen, T. (2007). p62/SQSTM1 binds directly to Atg8/LC3 to facilitate degradation of ubiquitinated protein aggregates by autophagy. J. Biol. Chem. *282*, 24131–24145.
15. Aparicio, R., Hansen, M., Walker, D.W., and Kumsta, C. (2020). The selective autophagy receptor SQSTM1/p62 improves lifespan and proteostasis in an evolutionarily conserved manner. Autophagy *16*, 772–774.
16. Kumsta, C., Chang, J.T., Lee, R., Tan, E.P., Yang, Y., Loureiro, R., Choy, E.H., Lim, S.H.Y., Saez, I., Springhorn, A., et al. (2019). The autophagy receptor p62/SQST-1 promotes proteostasis and longevity in C. elegans by inducing autophagy. Nat. Commun. *10*, 5648.
17. Aparicio, R., Rana, A., and Walker, D.W. (2019). Upregulation of the Autophagy Adaptor p62/SQSTM1 Prolongs Health and Lifespan in Middle-Aged Drosophila. Cell Rep. *28*, 1029–1040.e5.
18. Palikaras, K., Lionaki, E., and Tavernarakis, N. (2015). Coordination of mitophagy and mitochondrial biogenesis during ageing in C. elegans. Nature *521*, 525–528.
19. Johansen, T., and Lamark, T. (2011). Selective autophagy mediated by autophagic adapter proteins. Autophagy *7*, 279–296.
20. Zhang, B., Gong, J., Zhang, W., Xiao, R., Liu, J., and Xu, X.Z.S. (2018). Brain-gut communications via distinct neuroendocrine signals bidirectionally regulate longevity in C. elegans. Genes Dev. *32*, 258–270.
21. Antebi, A. (2013). Regulation of longevity by the reproductive system. Exp. Gerontol. *48*, 596–602.
22. Gelino, S., Chang, J.T., Kumsta, C., She, X., Davis, A., Nguyen, C., Panowski, S., and Hansen, M. (2016). Intestinal Autophagy Improves Healthspan and Longevity in C. elegans during Dietary Restriction. PLoS Genet. *12*, e1006135.
23. Lapierre, L.R., Gelino, S., Meléndez, A., and Hansen, M. (2011). Autophagy and lipid metabolism coordinately modulate life span in germline-less C. elegans. Curr. Biol. *21*, 1507–1514.
24. Wang, M.C., O'Rourke, E.J., and Ruvkun, G. (2008). Fat metabolism links germline stem

cells and longevity in C. elegans. Science *322*, 957–960.
25. Lapierre, L.R., Meléndez, A., and Hansen, M. (2012). Autophagy links lipid metabolism to longevity in C. elegans. Autophagy *8*, 144–146.
26. Chapin, H.C., Okada, M., Merz, A.J., and Miller, D.L. (2015). Tissue-specific autophagy responses to aging and stress in C. elegans. Aging (Albany NY) *7*, 419–434.
27. Ramachandran, P.V., Savini, M., Folick, A.K., Hu, K., Masand, R., Graham, B.H., and Wang, M.C. (2019). Lysosomal Signaling Promotes Longevity by Adjusting Mitochondrial Activity. Dev. Cell *48*, 685–696.e5.
28. Folick, A., Oakley, H.D., Yu, Y., Armstrong, E.H., Kumari, M., Sanor, L., Moore, D.D., Ortlund, E.A., Zechner, R., and Wang, M.C. (2015). Aging. Lysosomal signaling molecules regulate longevity in Caenorhabditis elegans. Science *347*, 83–86.
29. Seah, N.E., de Magalhaes Filho, C.D., Petrashen, A.P., Henderson, H.R., Laguer, J., Gonzalez, J., Dillin, A., Hansen, M., and Lapierre, L.R. (2016). Autophagy-mediated longevity is modulated by lipoprotein biogenesis. Autophagy *12*, 261–272.
30. O'Rourke, E.J., Soukas, A.A., Carr, C.E., and Ruvkun, G. (2009). C. elegans major fats are stored in vesicles distinct from lysosome-related organelles. Cell Metab. *10*, 430–435.
31. Lapierre, L.R., Silvestrini, M.J., Nuñez, L., Ames, K., Wong, S., Le, T.T., Hansen, M., and Meléndez, A. (2013). Autophagy genes are required for normal lipid levels in C. elegans. Autophagy *9*, 278–286.
32. Brooks, K.K., Liang, B., and Watts, J.L. (2009). The influence of bacterial diet on fat storage in C. elegans. PLoS One *4*, e7545.
33. Perez, C.L., and Van Gilst, M.R. (2008). A 13C isotope labeling strategy reveals the influence of insulin signaling on lipogenesis in C. elegans. Cell Metab. *8*, 266–274.
34. Kirkwood, T.B., and Holliday, R. (1979). The evolution of ageing and longevity. Proc. R. Soc. Lond. B Biol. Sci. *205*, 531–546.
35. Narbonne, P., and Roy, R. (2009). Caenorhabditis elegans dauers need LKB1/AMPK to ration lipid reserves and ensure long-term survival. Nature *457*, 210–214.
36. Miller, H., Fletcher, M., Primitivo, M., Leonard, A., Sutphin, G.L., Rintala, N., Kaeberlein, M., and Leiser, S.F. (2017). Genetic interaction with temperature is an important determinant of nematode longevity. Aging Cell *16*, 1425–1429.
37. Lapierre, L.R., Kumsta, C., Sandri, M., Ballabio, A., and Hansen, M. (2015). Transcriptional and epigenetic regulation of autophagy in aging. Autophagy *11*, 867–880.
38. Dupuy, D., Bertin, N., Hidalgo, C.A., Venkatesan, K., Tu, D., Lee, D., Rosenberg, J., Svrzikapa, N., Blanc, A., Carnec, A., et al. (2007). Genome-scale analysis of in vivo spatiotemporal promoter activity in Caenorhabditis elegans. Nat. Biotechnol. *25*, 663–668.
39. Kelmer Sacramento, E., Kirkpatrick, J.M., Mazzetto, M., Baumgart, M., Bartolome, A., Di Sanzo, S., Caterino, C., Sanguanini, M., Papaevgeniou, N., Lefaki, M., et al. (2020). Reduced proteasome activity in the aging brain results in ribosome stoichiometry loss and aggregation. Mol. Syst. Biol. *16*, e9596.
40. Guo, B., Huang, X., Zhang, P., Qi, L., Liang, Q., Zhang, X., Huang, J., Fang, B., Hou, W., Han, J., and Zhang, H. (2014). Genome-wide screen identifies signaling pathways that regulate autophagy during Caenorhabditis elegans development. EMBO Rep. *15*, 705–713.
41. Robichaud, S., Fairman, G., Vijithakumar, V., Mak, E., Cook, D.P., Pelletier, A.R., Huard, S., Vanderhyden, B.C., Figeys, D., Lavallée-Adam, M., et al. (2021). Identification of novel lipid droplet factors that regulate lipophagy and cholesterol efflux in macrophage foam cells. Autophagy *17*, 3671–3689.
42. Zhang, P., Na, H., Liu, Z., Zhang, S., Xue, P., Chen, Y., Pu, J., Peng, G., Huang, X., Yang, F., et al. (2012). Proteomic study and marker protein identification of Caenorhabditis elegans lipid droplets. Mol. Cell. Proteomics *11*, 317–328.
43. Vrablik, T.L., Petyuk, V.A., Larson, E.M., Smith, R.D., and Watts, J.L. (2015). Lipidomic and proteomic analysis of Caenorhabditis elegans lipid droplets and identification of ACS-4 as a lipid droplet-associated protein. Biochim. Biophys. Acta *1851*, 1337–1345.
44. Yang, L., Liang, J., Lam, S.M., Yavuz, A., Shui, G., Ding, M., and Huang, X. (2020). Neuronal lipolysis participates in PUFA-mediated neural function and neurodegeneration. EMBO Rep. *21*, e50214.
45. Zechner, R., Kienesberger, P.C., Haemmerle, G., Zimmermann, R., and Lass, A. (2009). Adipose triglyceride lipase and the lipolytic catabolism of cellular fat stores. J. Lipid Res. *50*, 3–21.
46. Lee, J.H., Kong, J., Jang, J.Y., Han, J.S., Ji, Y., Lee, J., and Kim, J.B. (2014). Lipid droplet protein LID-1 mediates ATGL-1-dependent lipolysis during fasting in Caenorhabditis elegans. Mol. Cell Biol. *34*, 4165–4176.
47. Olzmann, J.A., and Carvalho, P. (2019). Dynamics and functions of lipid droplets. Nat. Rev. Mol. Cell Biol. *20*, 137–155.
48. Denzel, M.S., Lapierre, L.R., and Mack, H.I.D. (2019). Emerging topics in C. elegans aging research: Transcriptional regulation, stress response and epigenetics. Mech. Ageing Dev. *177*, 4–21.
49. Moldavski, O., Amen, T., Levin-Zaidman, S., Eisenstein, M., Rogachev, I., Brandis, A., Kaganovich, D., and Schuldiner, M. (2015). Lipid Droplets Are Essential for Efficient Clearance of Cytosolic Inclusion Bodies. Dev. Cell *33*, 603–610.
50. Mejhert, N., Kuruvilla, L., Gabriel, K.R., Elliott, S.D., Guie, M.A., Wang, H., Lai, Z.W., Lane, E.A., Christiano, R., Danial, N.N., et al. (2020). Partitioning of MLX-Family Transcription Factors to Lipid Droplets Regulates Metabolic Gene Expression. Mol. Cell *77*, 1251–1264.e9.
51. Zhang, S.O., Box, A.C., Xu, N., Le Men, J., Yu, J., Guo, F., Trimble, R., and Mak, H.Y. (2010). Genetic and dietary regulation of lipid droplet expansion in Caenorhabditis elegans. Proc. Natl. Acad. Sci. USA *107*, 4640–4645.
52. Zaarur, N., Desevin, K., Mackenzie, J., Lord, A., Grishok, A., and Kandror, K.V. (2019). ATGL-1 mediates the effect of dietary restriction and the insulin/IGF-1 signaling pathway on longevity in C. elegans. Mol. Metab. *27*, 75–82.
53. Olzmann, J.A., Richter, C.M., and Kopito, R.R. (2013). Spatial regulation of UBXD8 and p97/VCP controls ATGL-mediated lipid droplet turnover. Proc. Natl. Acad. Sci. USA *110*, 1345–1350.
54. Wu, X., and Rapoport, T.A. (2018). Mechanistic insights into ER-associated protein degradation. Curr. Opin. Cell Biol. *53*, 22–28.
55. Bug, M., and Meyer, H. (2012). Expanding into new markets–VCP/p97 in endocytosis and autophagy. J. Struct. Biol. *179*, 78–82.
56. Hill, S.M., Wrobel, L., Ashkenazi, A., Fernandez-Estevez, M., Tan, K., Bürli, R.W., and Rubinsztein, D.C. (2021). VCP/p97 regulates Beclin-1-dependent autophagy initiation. Nat. Chem. Biol. *17*, 448–455.
57. Vembar, S.S., and Brodsky, J.L. (2008). One step at a time: endoplasmic reticulum-associated degradation. Nat. Rev. Mol. Cell Biol. *9*, 944–957.
58. Demishtein, A., Fraiberg, M., Berko, D., Tirosh, B., Elazar, Z., and Navon, A. (2017). SQSTM1/p62-mediated autophagy compensates for loss of proteasome polyubiquitin recruiting capacity. Autophagy *13*, 1697–1708.
59. Korolchuk, V.I., Mansilla, A., Menzies, F.M., and Rubinsztein, D.C. (2009). Autophagy inhibition compromises degradation of ubiquitin-proteasome pathway substrates. Mol. Cell *33*, 517–527.
60. Mohri-Shiomi, A., and Garsin, D.A. (2008). Insulin signaling and the heat shock response modulate protein homeostasis in the Caenorhabditis elegans intestine during infection. J. Biol. Chem. *283*, 194–201.
61. McColl, G., Roberts, B.R., Pukala, T.L., Kenche, V.B., Roberts, C.M., Link, C.D., Ryan, T.M., Masters, C.L., Barnham, K.J., Bush, A.I., and Cherny, R.A. (2012). Utility of an improved model of amyloid-beta (Abeta(1)(-)(4)(2)) toxicity in Caenorhabditis elegans for drug screening for Alzheimer's disease. Mol. Neurodegener. *7*, 57.
62. Franz, A., Ackermann, L., and Hoppe, T. (2014). Create and preserve: proteostasis in development and aging is governed by Cdc48/p97/VCP. Biochim. Biophys. Acta *1843*, 205–215.
63. Roberts, M.A., and Olzmann, J.A. (2020). Protein Quality Control and Lipid Droplet Metabolism. Annu. Rev. Cell Dev. Biol. *36*, 115–139.
64. Bersuker, K., and Olzmann, J.A. (2017). Establishing the lipid droplet proteome: Mechanisms of lipid droplet protein targeting and degradation. Biochim. Biophys. Acta. Mol. Cell Biol. Lipids *1862*, 1166–1177.
65. Galluzzi, L., Bravo-San Pedro, J.M., Levine, B., Green, D.R., and Kroemer, G. (2017). Pharmacological modulation of autophagy: therapeutic potential and persisting obstacles. Nat. Rev. Drug Discov. *16*, 487–511.
66. Zaffagnini, G., Savova, A., Danieli, A., Romanov, J., Tremel, S., Ebner, M., Peterbauer, T., Sztacho, M., Trapannone, R., Tarafder, A.K., et al. (2018). Phasing out the bad-How SQSTM1/p62 sequesters ubiquitinated proteins for degradation by autophagy. Autophagy *14*, 1280–1282.
67. Baskoylu, S.N., Chapkis, N., Unsal, B., Lins, J., Schuch, K., Simon, J., and Hart, A.C. (2022). Disrupted autophagy and neuronal dysfunction in C. elegans knockin models of FUS amyotrophic lateral sclerosis. Cell Rep. *38*, 110195.
68. Zaffagnini, G., Savova, A., Danieli, A., Romanov, J., Tremel, S., Ebner, M., Peterbauer, T., Sztacho, M., Trapannone, R., Tarafder, A.K., et al. (2018). p62 filaments capture and present ubiquitinated cargos for autophagy. EMBO J. *37*, e98308.
69. Hansen, M., Flatt, T., and Aguilaniu, H. (2013). Reproduction, fat metabolism, and life

span: what is the connection? Cell Metab. *17*, 10–19.

70. Silvestrini, M.J., Johnson, J.R., Kumar, A.V., Thakurta, T.G., Blais, K., Neill, Z.A., Marion, S.W., St Amand, V., Reenan, R.A., and Lapierre, L.R. (2018). Nuclear Export Inhibition Enhances HLH-30/TFEB Activity, Autophagy, and Lifespan. Cell Rep. *23*, 1915–1921.
71. Littlejohn, N.K., Seban, N., Liu, C.C., and Srinivasan, S. (2020). A feedback loop governs the relationship between lipid metabolism and longevity. Elife *9*, e58815.
72. Ding, L., Sun, W., Balaz, M., He, A., Klug, M., Wieland, S., Caiazzo, R., Raverdy, V., Pattou, F., Lefebvre, P., et al. (2021). Peroxisomal beta-oxidation acts as a sensor for intracellular fatty acids and regulates lipolysis. Nat. Metab. *3*, 1648–1661.
73. Schmitz, G., and Grandl, M. (2008). Lipid homeostasis in macrophages - implications for atherosclerosis. Rev. Physiol. Biochem. Pharmacol. *160*, 93–125.
74. Marschallinger, J., Iram, T., Zardeneta, M., Lee, S.E., Lehallier, B., Haney, M.S., Pluvinage, J.V., Mathur, V., Hahn, O., Morgens, D.W., et al. (2020). Lipid-droplet-accumulating microglia represent a dysfunctional and proinflammatory state in the aging brain. Nat. Neurosci. *23*, 194–208.
75. Nguyen, T.B., Louie, S.M., Daniele, J.R., Tran, Q., Dillin, A., Zoncu, R., Nomura, D.K., and Olzmann, J.A. (2017). DGAT1-Dependent Lipid Droplet Biogenesis Protects Mitochondrial Function during Starvation-Induced Autophagy. Dev. Cell *42*, 9–21.e5.
76. Di Paolo, G., and Kim, T.W. (2011). Linking lipids to Alzheimer's disease: cholesterol and beyond. Nat. Rev. Neurosci. *12*, 284–296.
77. Inloes, J.M., Hsu, K.L., Dix, M.M., Viader, A., Masuda, K., Takei, T., Wood, M.R., and Cravatt, B.F. (2014). The hereditary spastic paraplegia-related enzyme DDHD2 is a principal brain triglyceride lipase. Proc. Natl. Acad. Sci. USA *111*, 14924–14929.
78. Nuriel, T., Angulo, S.L., Khan, U., Ashok, A., Chen, Q., Figueroa, H.Y., Emrani, S., Liu, L., Herman, M., Barrett, G., et al. (2017). Neuronal hyperactivity due to loss of inhibitory tone in APOE4 mice lacking Alzheimer's disease-like pathology. Nat. Commun. *8*, 1464.
79. Labbadia, J., and Morimoto, R.I. (2015). The biology of proteostasis in aging and disease. Annu. Rev. Biochem. *84*, 435–464.
80. Brenner, S. (1974). The genetics of Caenorhabditis elegans. Genetics *77*, 71–94.
81. Stiernagle, T. (2006). Maintenance of C. elegans (WormBook), pp. 1–11.
82. Kamath, R.S., Fraser, A.G., Dong, Y., Poulin, G., Durbin, R., Gotta, M., Kanapin, A., Le Bot, N., Moreno, S., Sohrmann, M., et al. (2003). Systematic functional analysis of the Caenorhabditis elegans genome using RNAi. Nature *421*, 231–237.
83. Hansen, M., Hsu, A.L., Dillin, A., and Kenyon, C. (2005). New genes tied to endocrine, metabolic, and dietary regulation of lifespan from a Caenorhabditis elegans genomic RNAi screen. PLoS Genet. *1*, 119–128.
84. Holdorf, A.D., Higgins, D.P., Hart, A.C., Boag, P.R., Pazour, G.J., Walhout, A.J.M., and Walker, A.K. (2020). WormCat: An Online Tool for Annotation and Visualization of Caenorhabditis elegans Genome-Scale Data. Genetics *214*, 279–294.

STAR★METHODS

KEY RESOURCES TABLE

REAGENT or RESOURCE	SOURCE	IDENTIFIER
Antibodies		
Anti-ubiquitin (Mouse Monoclonal)	ThermoFisher	MAI-10035
Anti-actin (Mouse Monoclonal)	Millipore Sigma	MAB1501R
Anti-GFP (Rabbit Polyclonal)	Santa Cruz	sc-8334
Critical commercial assays		
SuperSignal West Femto Maximum Sensitivity Substrate	ThermoFisher	34096
iTaQ Universal SYBR Green Supermix	Bio-Rad	172-5124
Deposited data		
RNA sequencing	NCBI GEO	GEO204953
Experimental models: Organisms/strains		
C. elegans	See Tables S5 and S6 for details	
Oligonucleotides		
qPCR primers	See Table S7 for details	
Recombinant DNA		
C. elegans Ahringer RNAi Library	Source BioScience	
Software and algorithms		
ImageJ	NIH	
Prism 7	GraphPad	
Zen	Zeiss	
Stata	StataCorp	
Other		
Fluorescence Stereomicroscope V20 Discovery	Zeiss	
ChemiDoc Imaging System	Bio-Rad	
LightCycler 96	Roche	
Inverted Confocal Laser Scanning Microscope FV 3000	Olympus	

RESOURCE AVAILABILITY

Lead contact

Further information should be directed to and will be fulfilled by the lead contact, Prof. Louis R. Lapierre (louis.rene.lapierre@umoncton.ca).

Materials availability

Requests for strains should be directed to and will be fulfilled by the lead contact, Prof. Louis R. Lapierre (louis.rene.lapierre@umoncton.ca).

Data and code availability

RNA sequencing data are accessible on NCBI GEO (Accession number: GEO204953).

EXPERIMENTAL MODEL AND STUDY PARTICIPANTS

C. elegans strain maintenance

Nematodes were maintained at 20°C on agar NGM plates seeded with OP50 *E. coli* unless otherwise noted, as previously described.[80] Synchronized populations were prepared using a sodium hypochlorite solution to collect eggs as previously described.[81] Tables S5 and S6 contains the list of strains used in this study. HT115 *E. coli* and RNAi clones from the Ahringer library (Source Bioscience) were used for RNAi experiments.[82]

Transgenic strain construction

DNA constructs for the plasmids pLAP26 (*psqst-1::sqst-1::rfp::unc-54 3'UTR*) and pLAP29 (*psqst-1::sqst-1::gfp::rfp::unc-54 3'UTR*) were assembled using HiFi cloning and were injected into the germline of Day 1 adults (pLAP26 was co-injected with the pLAP7 (*myo-2::gfp::unc-54 3'UTR*)). Transgenic progeny was UV-irradiated for extrachromosomal array integration and selected for 100% transmission rate and backcrossed at least four times to wildtype N2. Details about strain construction are provided in Table S6.

METHOD DETAILS

Genome-wide RNAi screen

Approximately 50 synchronized transgenic eggs (*psqst-1::SQST-1::GFP*) were transferred onto plates seeded with RNAi against all genes from the Ahringer library (Source BioScience), which represents about 86% of the predicted genes in the *C. elegans* genome.[82] Nematodes were developed at 25°C and changes in GFP intensity or expression pattern were monitored on Day 1 of adulthood. As a negative control, bacteria expressing the L4440 backbone (i.e. empty vector) expressed in HT115 *E. coli* were used. The identity of each RNAi was not known to the scorer and fluorescence intensity was scored using a V20 dissection fluorescence microscope (Zeiss). Modifiers from the genome-wide RNAi screen were sequenced (GENEWIZ), validated three times and corroborated using transgenic animals expressing *SQST-1::RFP*. RNAi against the genes with the strongest effect on GFP expression were subsequently validated by silencing in adulthood only. Details are provided in Tables S1 and S2.

Lifespan analyses

Eggs obtained from bleaching were transferred onto OP50 *E. coli*. bacteria-seeded agar plates. All lifespan analyses were carried out at 25°C starting at Day 1 of adulthood after development at 20°C, unless otherwise noted. For gene knockdown experiments, worms were transferred to control bacteria expressing the empty vector (L4440) or expressing corresponding RNAi at day one of adulthood. Viability was scored every 1 to 3 days, as previously described.[83] Survival curves and statistical analyses (Mantel-Cox, log-rank) were generated using the Stata 15.0 software (StataCorp). Details are provided in Tables S3 and S4.

Comparative analyses

Knocked-down genes with the strongest effect on SQST-1::GFP levels were analyzed for gene ontology using WormCat[84] to identify which pathways were enriched. RNAi against genes that overlapped with the SQST-1 modulators, lipid droplet proteome,[43] and insoluble proteins[2] were then tested in adult-only experiments. Statistical significance of the overlap between any two groups of genes was calculated by hypergeometric probability (nemates.org, Lund laboratory, University of Kentucky). For adult-only RNAi validation, eggs from wild-type and SQST-1 transgenic animals were developed on OP50 *E coli*. bacteria at 20°C and transferred to corresponding RNAi plates at Day 1 of adulthood and grown at 25°C for an additional 72 hours. Adults were transferred away from their progeny and bright field and fluorescent images were taken daily.

Imaging and analyses

Worms were visualized using a Zeiss Discovery V20 fluorescence dissecting microscope (Zeiss, White Plains, NY). Worms were immobilized with 0.1% sodium azide in M9 solution (42 mM Na_2HPO_4 22 mM KH_2PO_4 86 mM NaCl, 1 mM $MgSO_4$-$7H_2O$) on agar plates and images were taken via Zen imaging software, using consistent parameters (magnification and exposure) within each experiment. For quantification of fluorescent signal, total fluorescence of each worm in each image was analyzed using ImageJ software and averaged for mean total fluorescence. Confocal microscopy images were obtained on an Olympus FV3000 inverted confocal laser scanning microscope (Leduc Bioimaging Facility, Brown University). Quantification of autophagosomes marked by GFP and mCherry showing yellow puncta and autolysosomes marked with only mCherry as GFP is quenched in acidic pH showing up as red puncta in the LGG-1 tandem reporter strain was carried out by color thresholding composite images for yellow or red puncta followed by counting the thresholded puncta using particle analysis on ImageJ. The overlap between lipid droplet protein (DHS-3) and tagged SQST-1 in the over-expressing strain was also performed using color thresholding followed by particle analysis functions in ImageJ (NIH).

Lipid staining

Worms were collected and washed twice with M9 solution and then fixed with 60% isopropanol for 30 minutes. After fixation, worms were stained overnight on a rocker with freshly prepared 60% Oil Red O (stock solution of 0.5% ORO in isopropanol diluted with water, equilibrated overnight on a rocker, and gravity-filtered). The following day, worms were washed with TBS-T (50 mM Tris base, 150 mM Tris HCl, 1.5 M NaCl, and 0.05% Tween-20), imaged using a Zeiss Discovery V20 fluorescence dissecting stereomicroscope and quantified with ImageJ (NIH).

Gene expression analysis

RNA was extracted from approximately 3,000 Day 1 worms and cDNA was prepared as previously described.[8] Gene expression levels were measured in biological triplicates using iTaq Universal SYBR Green Supermix (BIO-RAD) and a Roche LightCycler 96 (Indianapolis, IN).

Expression was normalized using two housekeeping genes, *act-1* and *cyn-1* and statistical analyses were performed using Prism 7 (GraphPad Software). See Table S7 for qPCR primers details.

RNAseq sample preparation and analysis

WT or *daf-2* mutant worms were developed on OP50 at 20°C and transferred to corresponding RNAi plates at Day 1 of adulthood and grown at 25°C for an additional 96 hours. Worms over-expressing ATGL-1::GFP were developed on OP50 at 20°C and grown at 25°C for an additional 96 hours. Adults were transferred away from their progeny daily. RNA was extracted and cDNA was prepared as previously described.[8] RNA quality was confirmed by BioAnalyzer (Genomics Core, Brown University), and *atgl-1* silencing was confirmed by qPCR before submitting samples for RNAseq analysis by GENEWIZ as previously described.[8]

Lipid droplet fractionation

Lipid droplets were isolated by ultracentrifugation from 24,000 Day 5 animals grown at 25°C on RNAi for 96 hours. Worms were homogenized with a ball-bearing homogenizer in MSB buffer (250 mM sucrose and 10 mM Tris-HCl pH 7.4) containing protease inhibitor (Roche). The lysate was cleared of cuticle debris and unlysed worms by centrifuging at 500 x g for 5 minutes. 10% of the cleared lysate was reserved as "Input". Nuclei and non-lipid droplet organelles were pelleted out of the cytosol by an ultracentrifugation spin at 45,000 RPM in a TLA100.1 rotor for 30 minutes at 4°C. The lipid droplet layer at the top of the centrifugation tube was aspirated, and contaminating organelles were removed by an additional centrifugation of the lipid droplet fraction. The final volume of lipid droplet and cytosol fractions were kept consistent across conditions.

Immunoblotting

Protein lysates were collected from worms using RIPA buffer (50 mM Tris-HCl, 250 mM sucrose, 1 mM EDTA, and Roche protease inhibitor tablet, with 1% or 5% SDS) and a handheld homogenizer, and cleared lysate protein concentrations were quantified using the DC Protein Assay kit (BIO-RAD). Equal amounts of total protein (10 μg) or comparative volumes for lipid droplet fractions (Input volume is 10% of lipid droplet and cytosol fractions) were separated by SDS-PAGE on a 4-15% Tris-Glycine gel and transferred to nitrocellulose. The membrane was briefly stained with Ponceau S to confirm even transfer, rinsed with TBS-T until clear, blocked with 5% nonfat dry milk in TBS-T, and immunoblotted with anti-Ubiquitin (ThermoFisher MAI-10035), anti-GFP (Santa Cruz SC-8334), and anti-Actin (Milllipore, MAB1501R). The membrane was developed using SuperSignal West Femto Maximum Sensitivity Substrate (ThermoFisher) and imaged on a ChemiDoc Imaging System (BIO-RAD).

QUANTIFICATION AND STATISTICAL ANALYSIS

Statistical analyses were performed using Prism 7 (GraphPad). When relevant, and as noted in the corresponding figure legend, *t-test* or ANOVA analyses were performed and standard deviations (SD) were shown. Statistical analyses for lifespan analyses were performed with Stata 15.0 software (StataCorp) using Mantel-Cox log-rank. Details are provided in Tables S3 and S4.